Available online at www.sciencedirect.com
ScienceDirect
Ceramics International 38 (2012) 701–706
CERAMICS INTERNATIONAL
www.elsevier.com/locate/ceramint

The doping concentration dependent tunable yellow luminescence of $Sr_5(PO_4)_2(SiO_4)$:Eu^{2+}

Xigang Wang [a], Jiuhui Gan [a], Yanlin Huang [a,*], Hyo Jin Seo [b,*]

[a] College of Chemistry, Chemical Engineering and Materials Science, Soochow University, Suzhou 215123, China
[b] Department of Physics, Pukyong National University, Busan 608-737, Republic of Korea

Received 24 June 2011; received in revised form 24 July 2011; accepted 25 July 2011

Abstract

Color tunable yellow-emitting phosphors of $Sr_{5-5x}Eu_{5x}(PO_4)_2SiO_4$ (x = 0.05–0.15) were prepared by conventional solid-state reaction method. The X-ray powder diffraction patterns, the photoluminescence excitation and emission spectra were measured. The main excitation bands of the phosphors locate at a broad band extending from 300 to 500 nm, which can match the emission of ultraviolet- and blue-emitting diode chips. The tunable luminescence color was realized by the changing Eu^{2+} doping in $Sr_5(PO_4)_2SiO_4$. The structure and luminescence properties were investigated. $Sr_{5-5x}(PO_4)_2SiO_4$:Eu_{5x} displays two typical luminescence centers, which originate from two different Sr^{2+} (Eu^{2+}) sites in the host. The site-occupation, the luminescence intensity and energy transfer between the Eu^{2+} ions occupying two different crystallographic Sr^{2+} sites were discussed on the base of the luminescence spectra and crystal structure. This is helpful to improve this phosphor for a potential application as a white light emitting diode phosphor.

Keywords: C. Optical properties; Luminescence; Apatite; White light emitting diode

1. Introduction

The luminescent properties of Eu^{2+}-doped solids have been intensively investigated in many kinds of hosts during the past decades [1–3]. In recent years, Eu^{2+}-doped phosphors have attracted further attentions for their significant applications in white light-emitting diodes (W-LEDs) because they absorb ultraviolet or blue (380–460 nm) light from LED chips and efficiently emit visible light [4–10]. The color temperature is important for the lighting of W-LEDs and it becomes an important challenge for improving white light [11].

The luminescence spectra of Eu^{2+}-doped apatite and its variations with the formula of $M_{10}(PO_4)_6X_2$ (M = Ca, Sr, Ba; $X = F^-, Cl^-, Br^-, OH^-$) have been extensively studied [12]. For example, $Sr_5(PO_4)_3(Cl,F)$:Eu^{2+} is an efficient phosphor for compact fluorescent lamp [13,14]. Eu^{2+}-doped $Ba_5(PO_4)_3Cl$:Eu^{2+} is a promising material for X-ray imaging [15]. Phosphors with apatite-structure have recently been confirmed to be suitable for field-emission displays (FEDs) and W-LEDs because of their low price, environmental friendliness, and thermal stability [16].

Apatite structure can be modified by a wide range of cationic and anionic substitutions [17]. For example, in $Sr_{10}(PO_4)_6X_2$ ($X = F^-, Cl^-, Br^-, OH^-$) lattice, the substitutions of $(SiO_4)^{4-} \rightarrow (PO_4)^{3-} + X^-$ is possible. The X^- content goes down with increasing $(SiO_4)^{4-}$ substitution because of the difference in effective charges between $(PO_4)^{3-}$ and $(SiO_4)^{4-}$ groups. The composition $Sr_5(PO_4)_2(SiO_4)$ need not to have any halogen. Blasse et al. reported the luminescence spectra and the energy transfer of the non-equivalent Eu^{2+} sites in $Sr_5(PO_4)_2SiO_4$ [18]. Recently, it has been confirmed that $Sr_5(PO_4)_2(SiO_4)$:Eu^{2+} has a potential application as a W-LEDs phosphor due to its efficient luminescence and an excellent thermal stability on temperature quenching [19].

In apatite structure, the $(SiO_4)^{4-}$ substitution has a great influence on the luminescence properties of Eu^{2+} ions. For example, the photoionization of Eu^{2+} ions in $Ba_{10}(PO_4)_6Cl_2$ can be enhanced with increasing substitution of $(SiO_4)^{4-}$ for $(PO_4)^{3-}$. This is attributed to the rigid covalent surroundings of

---

* Corresponding authors.
E-mail addresses: Huang@suda.edu.cn (Y. Huang), hjseo@pknu.ac.kr (H.J. Seo).

0272-8842/$36.00 © 2011 Elsevier Ltd and Techna Group S.r.l. All rights reserved.
doi:10.1016/j.ceramint.2011.07.059

the $(SiO_4)^{4-}$ network enhancing the scope for electron transfer reaction leading to the enhancement of the photo-ionization process [12]. Usually, the luminescence spectra of Eu^{2+}-doped apatite present the narrow blue bands corresponding to the $4f^65d^1 \rightarrow 4f^7(^8S_{7/2})$ allowed electric dipole transition, e.g., $Sr_5(PO_4)_3F:Eu^{2+}$ (440 nm) [20], $Sr_5(PO_4)_3Cl:Eu^{2+}$ (445 nm or 447 nm) [21,22]. In comparison with Eu^{2+}-doped apatite phosphates, the emission bands of Eu^{2+}-doped $Sr_5(PO_4)_2SiO_4$ shift to longer wavelength at 495 and 560 nm. The red-shift of emission band has been explained by the influence of substitution of silicate groups for phosphates with increasing structural disorder.

In this work, the luminescence properties of Eu^{2+}-doped $Sr_5(PO_4)_2SiO_4$ were further investigated. The X-ray powder diffraction and the detailed emission and excitation spectra were measured in the samples with the different Eu^{2+} doping. The dependence of luminescence colors and the excitation spectra on Eu^{2+}-doping were investigated. The spectroscopic results are discussed in relation to the existence of different crystallographic sites in Eu^{2+}-doped $Sr_5(PO_4)_2SiO_4$.

2. Experimental

The phosphors of $Sr_{5-5x}Eu_{5x}(PO_4)_2SiO_4$ ($x = 0.005$, 0.03, 0.05, 0.07, 0.1, 0.13, 0.15) were prepared by conventional solid-state reaction method. The starting materials were $SrCO_3$ (99.99%), $NH_4H_2PO_4$ (99.99%), SiO_2 (99.99%), and Eu_2O_3 (99.99%). The stoichiometric chemicals were weighed and thoroughly mixed in an agate mortar, then transferred to a corundum crucible and heated at 350 (in air), 850 (in air) and 1300 °C (in reductive atmosphere) for 15 h, respectively.

The phase purity was checked by powder X-ray diffraction (XRD) analysis collected on a Rigaku D/Max diffractometer operating at 40 kV, 30 mA with Bragg–Brentano geometry using Cu Kα radiation ($\lambda = 1.5405$ Å). The photoluminescence excitation and emission spectra were recorded on a Perkin-Elmer LS-50B luminescence spectrometer.

3. Results and discussion

3.1. The phase formation and crystal structure

All the samples were checked by powder XRD measurements. Fig. 1 shows the XRD patterns of $Sr(PO_4)_2SiO_4:Eu_{5x}$ ($x = 0.005$, 0.05, 0.07, 0.1, 0.13, 0.15). All the samples except for $Sr_{5-5x}Eu_{5x}(PO_4)_2SiO_4$ ($x = 0.13$, 0.15) are in good agreement with the JCPDs files No.21-1187 of $Sr_5(PO_4)_2SiO_4$, indicating a $Sr_5(PO_4)_2SiO_4$ single phase structure. In the Eu^{2+}-heavily doped samples ($x = 0.13$, 0.15) another impurity phase of $Sr_2P_2O_7$ (JCPDs No. 21-1187) was created. The syntheses of these two samples were repeated for three times. The results indicated that the impurity phase of $Sr_2P_2O_7$ always appeared when the doping of Eu^{2+} exceeded 13 mol%.

$Sr_5(PO_4)_2(SiO_4)$ is isostructural with $Sr_5(PO_4)_3(Cl,F)$, which crystallizes in the well-known apatite structure in the space group *P6₃/m* with $Z = 2$ [18]. In this apatite-like structure, there are two non-equivalent crystallographic sites for the Sr, namely Sr1 (Sr in a column) at $z = 0$ and 3/4, and Sr2 (Sr screw axis) at $z = 1/4$ and 3/4 [23,24]. Fig. 2 illustrates schematic views of the $Sr_5(PO_4)_2(SiO_4)$ structure along c-direction and the comparison

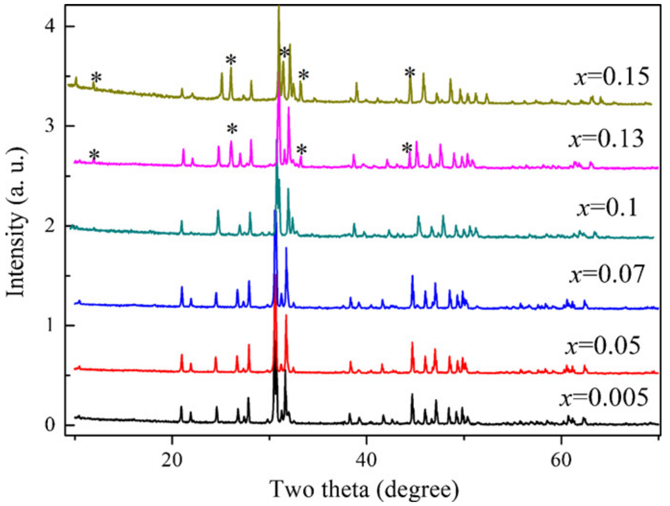

Fig. 1. XRD patterns of $Sr_{5-5x}Eu_{5x}(PO_4)_2SiO_4$ ($x = 0.005$, 0.05, 0.07, 0.1, 0.13, 0.15) prepared by solid-state reaction. * denotes the impurity phase of $Sr_2P_2O_7$.

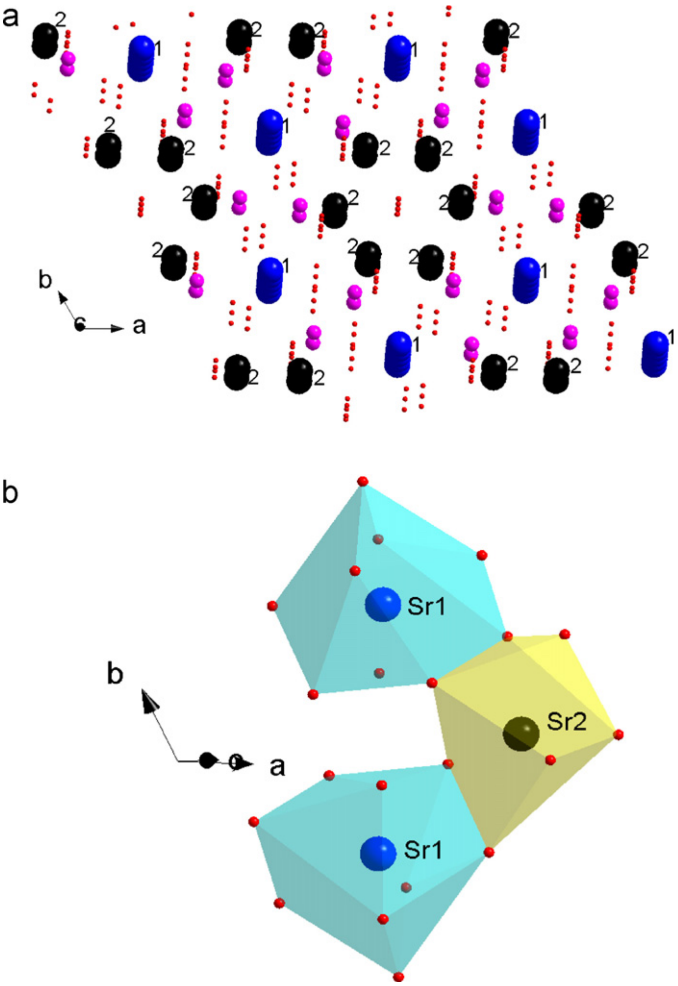

Fig. 2. (a) The schematic views of $Sr_5(PO_4)_2SiO_4$ structure along c-direction, the numbers "1" and "2" denote Sr1 and Sr2, respectively. (b) The comparison of the coordination geometries around the Sr1 and Sr2.

of the coordination geometries around the Sr1 and Sr2. The sites Sr1, occupy 4*f* Wyckoff position (C_3 point symmetry) with 9-fold coordination. And the site Sr2 is at the 6*h* Wyckoff position (C_s symmetry) with 7-fold coordination. This apatite structure can be represented as $[Sr1]_4[Sr2]_6(PO_4)_4(SiO_4)_2$. The ionic radii of Eu^{2+} ions are $r = 1.2$ Å (coordination number CN = 7) and $r = 1.3$ Å (CN = 9). The Sr^{2+} ions have bigger radii of $r = 1.35$ Å (CN = 7) and $r = 1.45$ Å (CN = 9) [25]. Therefore, Eu^{2+} ions should occupy statistically both Sr1 and Sr2 cation positions in the $Sr_5(PO_4)_2(SiO_4)$ lattices.

3.2. The luminescence emission and excitation spectra

Fig. 3(a) shows the luminescence spectra of $Sr_{5-5x}Eu_{5x}(PO_4)_2SiO_4$ ($x = 0.005$–0.15) under the excitation of 395 nm. The dependence of the total experimental luminescence intensity on the Eu^{2+} doping concentrations is shown in inset in Fig. 3(b). The luminescence intensity of $Sr_{5-5x}Eu_{5x}(PO_4)_2(SiO_4)$ increases with increasing the Eu^{2+}-doping until a maximum intensity about $x = 0.05$ is reached, and then it decreases because of conventional concentration quenching process [19].

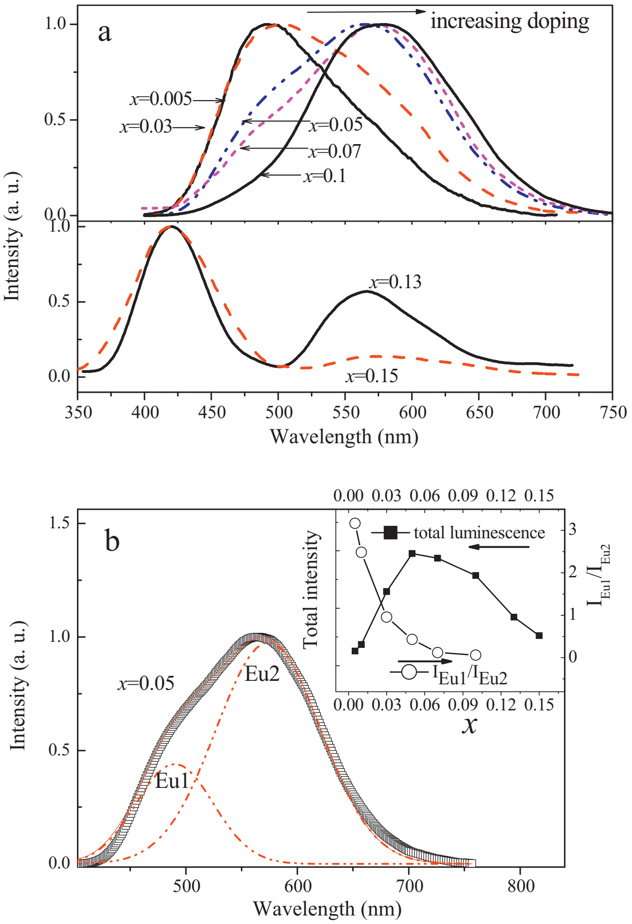

Fig. 3. (a) The normalized luminescence spectra of $Sr_{5-5x}Eu_{5x}(PO_4)_2SiO_4$ ($x = 0.005$, 0.03, 0.05, 0.07, 0.1, 0.13, 0.15) under the excitation of 395 nm. (b): a representative deconvoluted emission spectrum (x = 0.05), the insets are the dependence of the total experimental luminescence intensity on the Eu^{2+} doping concentrations and the relative intensity ratio between Eu1 and Eu2: I_{Eu1}/I_{Eu2}.

The spectra of $Sr_{5-5x}Eu_{5x}(PO_4)_2SiO_4$ ($x = 0.005$, 0.03, 0.05, 0.07, 0.1) display a broad emission band from 400 to 700 nm ascribed to $4f^65d^1 \rightarrow 4f^7(^8S_{7/2})$ transitions of Eu^{2+} ions. However, the luminescence spectra of $Sr_{5-5x}Eu_{5x}(PO_4)_2SiO_4$ ($x = 0.13$, 0.15) show a abrupt change, which display two clearly separated emission bands at 420 nm and 580 nm. The blue emission band at 420 nm might be from $Sr_2P_2O_7:Eu^{2+}$ [26]. The mixed crystal phase of $Sr_2P_2O_7$ and $Sr_5(PO_4)_2SiO_4$ was observed in XRD results of $Sr_{5-5x}Eu_{5x}(PO_4)_2SiO_4$ ($x = 0.13$, 0.15) (Fig. 1).

The emission band of $Sr_{5-5x}Eu_{5x}(PO_4)_2SiO_4$ ($x = 0.005$, 0.03, 0.05, 0.07, 0.1) shows the obvious asymmetric shapes, indicating the existence of two different luminescent centers [19]. It can be clearly found in Fig. 3(a) that the luminescence intensities of Eu1 and Eu2 have great changes with increasing the Eu^{2+} doping. All the spectra could be reproduced as a superposition of at least two Gaussian components. Fig. 3(b) is the representative Gaussian fitting into two components peaked at 485 nm (Eu1) and 580 nm (Eu2) for the emission spectra of $Sr_{5-5x}Eu_{5x}(PO_4)_2SiO_4$ ($x = 0.05$). The relative intensity ratio between Eu1 and Eu2: I_{Eu1}/I_{Eu2} was calculated by the deconvoluted emission intensities from each spectra of $Sr_{5-5x}Eu_{5x}(PO_4)_2SiO_4$ ($x = 0.005$, 0.03, 0.05, 0.07, 0.1) and displayed in inset in Fig. 3(b). The contribution of the Eu^{2+} luminescence from the Eu2 becomes larger with increasing the Eu^{2+} doping. Blasse et al. ascribed this to the energy transfer from Eu1 to Eu2 [18]. Consequently, in Eu^{2+} doped $Sr_5(PO_4)_2SiO_4$, the emission red-shift was also observed from the high energy center of 480 nm to low energy center 540 nm with increasing of Eu^{2+} doping (Fig. 3(a)).

In the structure of $Sr_5(PO_4)_2SiO_4$, there are two non-equivalent sites as shown in Fig. 2(b). Sr1 ions occupy the 4f site surrounded by nine oxygen atoms with C_3 symmetry. The Sr2 ions in the 6 h site are surrounded by seven oxygen atoms with C_s symmetry [27,28]. The Sr2 is more distorted that that of Sr1. And the bond-length of Sr2–O is shorter than that of Sr1–O. Thus, in $Sr_{5-5x}Eu_{5x}(PO_4)_2SiO_4$ ($x = 0.005$, 0.03, 0.05, 0.07, 0.1) the high-energy emission at 485 nm (Eu1) originates from the Eu^{2+} ions which occupy loose crystal circumstance with larger Sr–O bond length (Sr1 site); and the low-energy emission at 580 nm (Sr2 site) are ascribed to the Eu^{2+} ions occupying compact crystal circumstance with shorter Sr2–O bond length (Sr2).

Fig. 4 shows the CIE chromaticity diagram for $Sr_{5-5x}Eu_{5x}(PO_4)_2SiO_4$ ($x = 0.005$, 0.03, 0.05, 0.07, 0.1, 0.13, 0.15). With increasing Eu^{2+}-content from $x = 0.005$–0.1, the emission changes in color from yellowish-green (0.387, 0.577) to deep-yellow (0.455, 0.493), which is consistent with the red-shift of emission spectra. $Sr_{5-5x}Eu_{5x}(PO_4)_2SiO_4$ ($x = 0.13$) and $Sr_{5-5x}Eu_{5x}(PO_4)_2SiO_4$ ($x = 0.15$) present white and blue luminescence, respectively. It is believed that this phosphor $Sr_{5-5x}Eu_{5x}(PO_4)_2SiO_4$ has the potential of being a color tunable W-LED material by adjusting the Eu^{2+} doping concentrations.

The white luminescence from a single phase in $Sr_{5-5x}Eu_{5x}(PO_4)_2SiO_4$ ($x = 0.13$) is very valuable. However, this phosphor presents weak luminescence intensity because of concentration quenching, and the exact content of the impurity of $Sr_2P_2O_7$ in

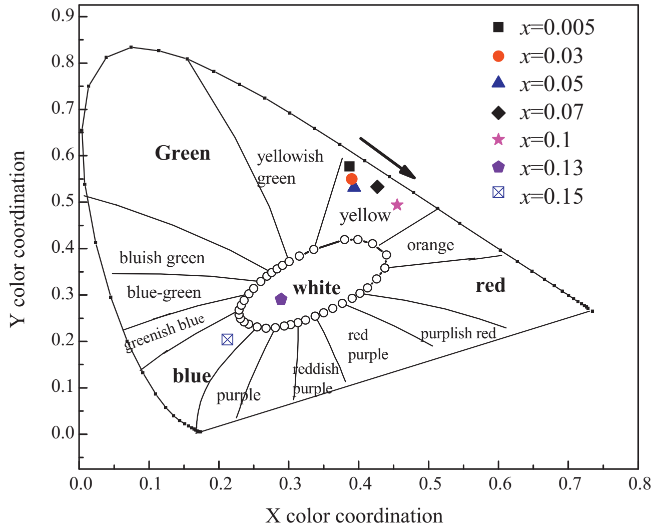

Fig. 4. CIE chromaticity coordinates of $Sr_{5-5x}Eu_{5x}(PO_4)_2SiO_4$ ($x = 0.005$–0.15)calculated from Fig. 3(a).

the synthesis is not easy to be controlled. Further experiments could be further investigated on this phenomenon.

The normalized excitation spectra of the emission bands at 485 nm and 580 nm are shown in Fig. 5(a) and (b), respectively, which consist of the broad absorption bands from 4*f*–5*d* transition of Eu^{2+} ions. The different excitation spectra in Fig. 5 for the two emission bands Eu1 and Eu2 testify the two distinct Eu^{2+} centers in $Sr_5(PO_4)_2SiO_4$. With increasing the Eu^{2+} doping, the excitation spectra move from near UV band around 400 nm to blue region around 450 nm. This indicates that the $Sr_{5-5x}Eu_{5x}(PO_4)_2SiO_4$ ($x = 0.005$, 0.03, 0.05, 0.07, 0.1, 0.13, 0.15) phosphors can well match with both the UV-LED (360–400 nm) and blue-LED chips (450 nm), which is essential for improving the efficiency of W-LEDs. The excitation spectra of $Sr_{5-5x}Eu_{5x}(PO_4)_2SiO_4$ is very different from the Eu^{2+} doped apatite phosphates, where the excitation of Eu^{2+} only presents absorption bands in the near UV (350–400 nm).

3.3. The luminescence characteristics of $Sr(PO_4)_2SiO_4$:Eu_{5x}

$Sr_5(PO_4)_2SiO_4$ has an apatite structure. In comparison with Eu^{2+}-doped apatite phosphates, the luminescence of $Sr_{5-5x}Eu_{5x}(PO_4)_2SiO_4$ ($x = 0.005$, 0.03, 0.05, 0.07, 0.1) have two distinct characteristics. Firstly, the emission spectra of Eu^{2+}-doped $Sr_5(PO_4)_2SiO_4$ are shifted to higher wavelength at 485 and 580 nm, which could be assigned to the Sr1 and Sr2 sites, respectively. Eu^{2+}-doped $Sr_5(PO_4)_2SiO_4$ shows yellowish-green to yellow luminescence color. However, the luminescence of Eu^{2+}-doped apatite phosphates only gives blue emission, e.g., $Sr_5(PO_4)_3F$:Eu^{2+} (440 nm) [20], $(Ca,Mg)_5(PO_4)_3Cl$:Eu^{2+} (458 nm) [16], $Sr_5(PO_4)_3Cl$:Eu^{2+} (445 nm or 447 nm) [21,29], and $Ca_5(PO_4)_3Cl$: Eu^{2+} (457 nm) [22].

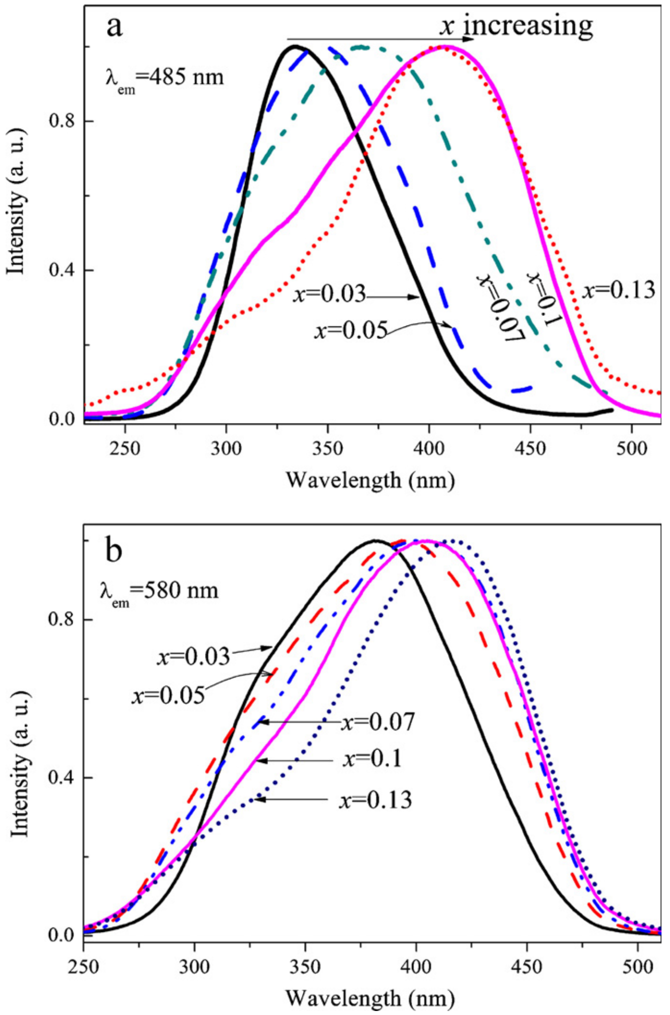

Fig. 5. The normalized excitation spectra of $Sr_{5-5x}Eu_{5x}(PO_4)_2SiO_4$ ($x = 0.03$, 0.05, 0.07, 0.1, 0.13) by monitoring the emission from 485 nm (a) and 580 nm (b).

Secondly, $Sr_{5-5x}Eu_{5x}(PO_4)_2SiO_4$ show two distinct emission bands and the luminescence wavelength positions have great red-shift from Eu1 to Eu2 with increasing of the Eu^{2+} doping levels. However, in Eu^{2+} doped apatite phosphates, the emission of Eu^{2+} show narrow emission band with nearly no shift, for example, the emission wavelength positions of $Ca_5(PO_4)_3F$:Eu^{2+} ($\lambda_{em} = 440$ nm), and $M_5(PO_4)_3Cl_x$:Eu^{2+} M = Ca (457 nm), Sr (447 nm) and Ba (436 nm) have not obvious dependence on the Eu^{2+} doping levels [22].

This can be explained by the influence of substitution of silicate groups for phosphates with increasing structural disorder. The lattice structure of $Sr_5(PO_4)_2PO_4$ can be evolved from $Sr_5(PO_4)_3(F,Cl)$ by the substitution: $SiO_4^{4-} = (PO_4)^{3-} + (F,Cl)^{-}$. In this substitution, some vacancies on original $(F,Cl)^{-}$ sites can be created. The $Sr_5(PO_4)_3(F,Cl)$ lattice is constituted by the $(PO_4)^{3-}$ tetrahedral and gives little distortion, while the $Sr_5(PO_4)_2SiO_4$ lattice is made of $(SiO_4)^{4-}$ and $(PO_4)^{3-}$ network giving rise to a considerable readjustment in the Si–O bond lengths. This is the main difference between these two cases. Thus the $Sr_5(PO_4)_2SiO_4$ lattice has a distorted site symmetry by the absence of mirror plane perpendicular (symmetry element/*m*) to the *c*-axis with the lattice symmetry lowered to P_6 accompanying the silicate substitution [29].

Jagannathan et al. [12] have suggested that when a part of the $(PO_4)^{3-}$ anionic network of the matrix is replaced by the more covalent $(SiO_4)^{4-}$ in apatite, a more covalent $(SiO_4)^{4-}$ may further suppress the lowest excited (the emitting state) state when compared to the $(PO_4)^{3-}$ only system. The Eu^{2+} ions experience stronger crystal field strength, leading to the emission maximum shifted to longer wavelengths.

Eu^{2+}-doped $Sr_5(PO_4)_3Cl$ is one of well known lamp phosphors. The luminescence quantum efficiency (QE) of $Sr_5(PO_4)_3Cl:Eu^{2+}$ is 85% under excitation of 254 nm [30]. Blasse et al. reported that the QE of $Sr_5(PO_4)_2SiO_4:Eu^{2+}$ is moderate (l0–15% for 254 nm excitation) [18]. This low QE values are due to the fact that 254 nm is not an efficient excitation wavelength (Fig. 5). A higher QE of $Sr_5(PO_4)_2SiO_4:Eu^{2+}$ could be expected under the excitation of near UV light about 400 nm. The new investigations for the QE values of $Sr_5(PO_4)_2SiO_4:Eu^{2+}$ with different Eu^{2+} doping will be conducted in the future.

4. Conclusions

In conclusion, $Sr_{5-5x}Eu_{5x}(PO_4)_2SiO_4$ ($x = 0.005–0.15$) phosphors have been prepared by high temperature solid-state reaction. The distinct characteristics of $Sr_5(PO_4)_2SiO_4:Eu^{2+}$ different from the Eu^{2+}-doped apatite phosphates were discussed. The $Sr_{5-5x}Eu_{5x}(PO_4)_2SiO_4$ ($x = 0.005–0.1$) display characteristic two-peak emission spectra with high energy emission band at 485 nm (Eu1) from Eu^{2+} at Sr1 site and the other one 580 nm (Eu2) red-shifted one from Eu^{2+} at Sr2 site. With increasing the Eu^{2+}-concentration below 10%, a red-shift in the emission band is observed from 485 nm (0.5% Eu^{2+}) (yellowish-green) to 580 nm (10% Eu^{2+}) (deep-yellow). This is ascribed to energy migration and energy transfer between the two Eu^{2+} sites. The relative contribution of Eu2 luminescence can be enhanced in a comparison with that of Eu1 with increasing the Eu^{2+} doping in $Sr_{5-5x}Eu_{5x}(PO_4)_2SiO_4$ ($x = 0.005–0.1$). Heavily Eu^{2+}-doped samples, $Sr_{5-5x}Eu_{5x}(PO_4)_2SiO_4$ ($x = 0.13$) and $Sr_{5-5x}Eu_{5x}(PO_4)_2SiO_4$ ($x = 0.15$), present white and blue luminescence, respectively. But these two samples present weak luminescence intensity because of concentration quenching. The excitation spectra $Sr_{5-5x}Eu_{5x}(PO_4)_2SiO_4$ ($x = 0.005–0.15$) display a broad wavelength region from 400 nm to 500 nm, matching with both the UV-LED chips and blue chips. $Sr_{5-5x}Eu_{5x}(PO_4)_2SiO_4$ phosphors have the potential of being a color tunable W-LED material by controlling the Eu^{2+} doping concentrations.

Acknowledgements

This work was supported by the Mid-career Researcher Program through National Research Foundation of Korea (NRF) grant funded by the Ministry of Education, Science and Technology (MEST) (Project No. 2009-0078682), and by A Project Funded by the Priority Academic Program Development of Jiangsu Higher Education Institutions (PAPD).

References

[1] P. Dorenbos, Energy of the first $4f^7 \rightarrow 4f^65d$ transition of Eu^{2+} in inorganic compounds, J. Lumin. 104 (2003) 239–260.

[2] P. Dorenbos, f → d transition energies of divalent lanthanides in inorganic compounds, J. Phys. Condens. Matter 15 (2003) 575–594.

[3] P. Dorenbos, Energy of the Eu^{2+} 5d state relative to the conduction band in compounds, J. Lumin. 128 (2008) 578–582.

[4] S.H. Lee, H.Y. Koo, Y.C. Kang, Characteristics of α'- and β-$Sr_2SiO_4:Eu^{2+}$ phosphor powders prepared by spray pyrolysis, Ceram. Inter. 36 (2010) 1233–1238.

[5] Y.C. Kang, H.S. Roh, H.D. Park, S.B. Park, Optimization of VUV characteristics and morphology of $BaMgAl_{10}O_{17}:Eu^{2+}$ phosphor particles in spray pyrolysis, Ceram. Inter. 29 (2003) 41–47.

[6] J.M. Kim, S.J. Park, K.H. Kim, H.W. Choi, The luminescence properties of $M_2MgSi_2O_7:Eu^{2+}$($M = Sr$, Ba) nano phosphor in ultraviolet light emitting diodes, Ceram. Inter. (2011), doi:10.1016/j.ceramint.2011.05.100.

[7] J.H. Kim, H.D. Jang, S.K. Kim, H.B. Lee, E.S. Kim, Photoluminescence and photocurrent characteristics of $Sr_{1-x}Ba_xAl_2O_4:Eu^{2+}$, Ni^{2+} phosphors, Ceram. Inter. (2011), doi:10.1016/j.ceramint.2011.05.101.

[8] Z. Shi, W. Yang, S. Bai, G. Qiao, Z. Jin, Preparation of Eu^{2+}-doped AlN phosphors by plasma activated sintering, Ceram. Inter. 37 (2011) 2051–2054.

[9] L. Chen, C.C. Lin, C.W. Yeh, R.S. Liu, Rare-earth activated nitride phosphors: synthesis, luminescence and applications, Materials 3 (2010) 2172–2195.

[10] C.C. Lin, R.S. Liu, Advances in phosphors for light-emitting diodes, J. Phys. Chem. Lett. 2 (2011) 1268–1277.

[11] V. Bachmann, C. Ronda, O. Oeckler, W. Schnick, A. Meijerink, Color point tuning for $(Sr,Ca,Ba)Si_2O_2N_2:Eu^{2+}$ for white light LEDs, Chem. Mater. 21 (2009) 316–325.

[12] R. Jagannathan, T.R.N. Kutty, Anomalous fluorescence features of Eu^{2+} in apatite-pyromorphite type matrices, J. Lumin. 71 (1997) 115–121.

[13] T. Welker, Recent developments on phosphors for fluorescent lamps and cathode-ray tubes, J. Lumin. 48–49 (1991) 49–56.

[14] M. Kottaisamy, R. Jagannathant, P. Jeyagopal, R.P. Rao, R.L. Narayanan, Eu^{2+} luminescence in $M_5(PO_4)_3X$ apatites, where M is Ca^{2+}, Sr^{2+} and Ba^{2+}, and X is F^-, Cl^-, Br^- and OH^-, J. Phys. D Appl. Phys. 27 (1994) 2210–2215.

[15] M. Sato, T. Tanakasi, M. Ohta, Photostimulated luminescence and structural characterization of $Ba_5(PO_4)_3Cl:Eu^{2+}$ phosphors, J. Electrochem. Soc. 141 (1994) 1851–1855.

[16] W.N. Wang, F. Iskandar, K. Okuyama, Y. Shinomiya, Rapid synthesis of non-aggregated fine chloroapatite blue phosphor powders with high quantum efficiency, Adv. Mater. 20 (2008) 3422–3426.

[17] Y. Shen, A. Tok, Z. Dong, Synthesis and crystal structure characterization of silicate apatite $Sr_2Y_8(SiO_4)_6O_2$, J. Am. Ceram. Soc. 93 (2010) 1176–1182.

[18] G. Blasse, A. Bril, Energy transfer between Eu^{2+} ions in nonequivalent sites in strontium-silicate-phosphate, Phys. Lett. A 28 (1969) 572–573.

[19] J. Gan, Y. Huang, L. Shi, X. Qiao, H.J. Seo, Luminescence properties of Eu^{2+}-activated $Sr_5(PO_4)_2(SiO_4)$ for green-emitting phosphor, Mater. Lett. 63 (2009) 2160–2162.

[20] I.M. Nagpure, K.N. Shinde, S.J. Dhoble, A. Kumar, Photoluminescence characterization of Dy^{3+} and Eu^{2+} ion in $M_5(PO_4)_3F$ ($M = Ba$, Sr, Ca) phosphors, J. Alloys Compd. 481 (2009) 632–638.

[21] Y. Song, H. You, M. Yang, Y. Zheng, K. Liu, G. Jia, Y. Huang, L. Zhang, H. Zhang, Facile synthesis and luminescence of $Sr_5(PO_4)_3Cl:Eu^{2+}$ nanorod bundles via a hydrothermal route, Inorg. Chem. 49 (2010) 1674–1678.

[22] X. Zhang, J. Zhang, J. Huang, X. Tang, M. Gong, Synthesis and luminescence of Eu^{2+}-doped alkaline-earth apatites for application in white LED, J. Lumin. 130 (2010) 554–559.

[23] L. Boyer, B. Piriou, J. Carpena, J.L. Lacout, Study of sites occupation and chemical environment of Eu^{3+} in phosphate-silicates oxyapatites by luminescence, J. Alloys Compd. 311 (2000) 143–152.

[24] D. NoÈtzold, H. Wulff, G. Herzog, Structural and optical properties of the system $(Ca,Sr,Eu)_5(PO_4)_3Cl$, Phys. Status Solidi (b) 191 (1995) 21–30.

[25] R.D. Shannon, Revised effective ionic radii and systematic studies of interatomic distances in halides and chalcogenides, Acta Crystallogr. A 32 (1976) 751–767.

[26] R. Pang, C. Li, L. Shi, Q. Su, A novel blue-emitting long-lasting proyphosphate phosphor $Sr_2P_2O_7$:Eu^{2+},Y^{3+}, J. Phys. Chem. Solids 70 (2009) 303–306.

[27] B. Piriou, D. Fahmi, J. Dexpert-Ghys, A. Taitai, J.L. Lacout, Unusual fluorescent properties of Eu^{3+} in oxyapatites, J. Lumin. 39 (1987) 97–103.

[28] K. Sudarsanan, R.A. Youner, Significant precision in crystal structural details holly springs hydroxyapatite, Acta Crystallogr. B 25 (1969) 1534–1543.

[29] K. Marimuthu, L.C. Nehru, A. Mani, R. Ramesh, G. Muralidharan, R. Jagannathan, Apatites and britholites, are they akin—as probed by Eu^{3+} luminescence? J. Phys. Condens. Matter 13 (2001) 537–547.

[30] Franz Kummer, in: C.W. Struck, K.C. Mishra, B. Di Bartolo (Eds.), The Production of Fluorescent Lamp Phosphors, Physics and Chemistry of Luminescent Materials, The Electrochemical Society, Inc., Pennington, NJ, USA, 1999, p. 211.